

The Mars Pathfinder Atmospheric Structure Investigation / Meteorology
(ASI/MET) experiment.

(7th November 1997)

J.T. Schofield, & D. Crisp, *Jet Propulsion Laboratory*,
J.R. Barnes, *Oregon State University*,
R.M. Haberle, *Ames Research Center*,
J.A. Magalhães, J.R. Murphy, and A. Seiff, *San Jose State University Foundation*
S. Larsen, *Risø National Laboratory - Denmark*.
G. Wilson, *Arizona State University*

Abstract

The Mars Pathfinder **ASI/MET** experiment measured the vertical density, pressure and temperature structure of the martian atmosphere from the surface to 160 km, and monitored surface meteorology and climate for 83 sols. Atmospheric structure and the weather record are similar to those observed by the Viking 1 lander (**VL- 1**) at the same latitude, altitude, and season 21 years ago, but there are differences related to diurnal effects and landing site surface properties. These include a cold nighttime upper atmosphere, 10-12 K warmer atmospheric temperatures near the surface, light slope-controlled winds, and dust devils identified by their pressure, wind, and temperature signatures. The results are consistent with the warm, moderately dusty atmosphere seen by **VL- 1**.

Introduction

The **ASI/MET** experiment consists of a suite of sensors designed to measure the vertical structure of the atmosphere during entry, descent, and landing (**EDL**), and to study **martian** surface meteorology and climate for the duration of the Pathfinder mission (1, 2) *In situ* vertical structure measurements have been made only twice by the Viking entry vehicles (3), both during the daytime. In addition to adding a third profile, **ASI/MET** provides the first nighttime observation, giving valuable information on the diurnal variation of vertical structure, particularly in the upper atmosphere which is inaccessible to existing remote sensing techniques. The vertical coverage and resolution are also superior to Viking (2,3). Both Viking landers obtained records of atmospheric pressure, temperature and wind velocity at the surface that extended over several Mars years. More recent earth-based, disk-averaged, microwave observations have been interpreted to indicate

episodic cooling of the **martian** lower atmosphere by about 20K relative to the conditions observed during the Viking mission (4). By continuing the Viking record, after 21 years, **ASI/MET** results are able to determine whether **martian** meteorology and climate have changed or **remained** stable in the late northern summer. Improved measurement sensitivity and temporal resolution (2), also reveal new phenomena not seen by Viking and, together with temperature measurements at three levels, give better information on the exchange of heat and momentum between the atmosphere and the surface.

The **ASI/MET** experiment combined accelerometer and MET instruments(2). The accelerometer instrument contained science and engineering accelerometers that each monitored accelerations along three orthogonal axes. In each axis, the maximum sensitivity was $20 \mu\text{m/s}^2$ (2×10^{-6} Earth g's), and the accelerations expected during EDL were covered by commendable measurement ranges of 16 mg, 800 mg, and 40 g full scale. The MET instrument consisted of pressure, temperature, and wind sensors. Pressure was measured by a Tavis variable reluctance aneroid barometer through a 1 m inlet tube which was exposed to the atmosphere during parachute descent as well as after landing (1). The pressure measurements have a maximum sensitivity of 0.25 μbar , more than a factor of 100 better than that available to the Viking landers (5). All the MET temperature and wind sensors are mounted on a 1.1 m high mast, deployed at the end of a lander petal to isolate it from spacecraft thermal contamination (1). Atmospheric temperature was **measured by four thin-wire thermocouples; one designed to measure temperature during parachute descent**, and three designed for surface boundary layer measurements 25, 50, and 100 cm above the base of the mast. All four thermocouples have time constants of 1 to 2 s and sensitivities of 0.01 K. Wind was **measured** by a six segment hot-wire sensor at the top of the mast, 1.1 m above the mast base. The wires are heated by a current passed in series through all six segments, and the temperature differences between low and high current modes for each segment are used to determine wind speed and direction.

The accelerometer and MET instruments recorded data continuously throughout EDL until about 1 minute after impact at approximately **03:00** local solar time (**LST**). Regular surface pressure, temperature, and wind measurements by the MET instrument began about 4 hours after impact at **07:00** LST on Sol 1, and the MET mast was deployed at **13:30** LST.

The science accelerometer detected the upper atmosphere 160 km above the landing site when the entry vehicle had a velocity of 7.4 km/see relative to the atmosphere and a flight path angle 14.8° below the local horizontal. 1.5 minutes later the entry vehicle experienced a peak deceleration of 15.9 Earth g's at an altitude of 33 km. After 3 minutes (9 km) the parachute **deployed** and at 3.4

minutes (7.4 km) the heat shield separated from the lander allowing the pressure sensor to begin unobstructed measurements of the atmosphere. The inflation of shock-absorbing airbags at 5.1 minutes (0.3 km) terminated the **unobstructed** pressure measurements, and descent rocket firing at 5.2 minutes (0.1 km) ended the direct measurement of aerodynamic decelerations. The first impact of the probe with the **martian** surface occurred **5.3** minutes after it entered the atmosphere. In the first minute after impact the lander **bounced** 15 times and pressure sensor data indicated that it rolled 10 m vertically downhill. It came to rest about a minute later at a site 3389.7 km from the center of mass of Mars (6). Surface acceleration measurements of $3.716 \text{ m}\cdot\text{s}^{-2}$ agree with values of $3.717 \text{ m}\cdot\text{s}^{-2}$ calculated for the lander location and height (7), providing a verification of accelerometer gain calibration.

Because the engineering accelerometers were used to control parachute deployment, and remained in their least sensitive 40 g scale, atmospheric profiles were derived from science accelerometer data only, which were logged at 32 Hz throughout EDL. MET pressure and temperature data were collected at 2 Hz during the parachute descent and landing phases of EDL. However, spacecraft design constraints did not allow the descent temperature sensor to be exposed to the free flow around the lander, so that direct atmospheric temperature measurements **were** not possible (2,8).

For the 30 day primary landed mission, 51 equally spaced MET measurement sessions were made **each day to monitor the atmospheric diurnal cycle and synoptic (day-to-day) variations. These three minute** sessions sampled the atmosphere at 4 second intervals, and were interspersed with 15 minute and 1 hour sessions of 1 second sampling to monitor the surface boundary layer. The boundary layer sessions were repeated as frequently as allowed by data volume, in a pattern that sampled all local times of day as rapidly as possible. Finally, on Sol 25, a 24 hour session was executed that sampled science data continuously at 4 second intervals for a complete daily cycle. The continuous MET observations desired during the primary mission were interrupted by spacecraft computer resets. One of these resets was associated with errors in MET software, and the measurements were limited to the nighttime from Sols 12-17, until the errors were corrected.

Entry, Descent, and Landing .

Atmospheric density, pressure and temperature profiles have been derived from ASI/MET deceleration measurements during Pathfinder EDL and compared with **VL- 1** results (Figs 1 &2). The mean solar forcing of the **martian** atmosphere at the time of the Pathfinder and **VL- 1** profiles was similar. Solar longitudes of **98° (VL- 1)** and 1420 (Pathfinder), correspond to a seasonal difference from mid to late summer, and to a smaller Mars-sun distance at the time of the

Pathfinder profile. Solar activity, as measured by sunspot counts, was near-minimum for both profiles, the lower atmosphere had comparable amounts of dust (10), and the two landings were at similar latitudes and longitudes *on* Mars. However, the different time of day (03:00 LST for Pathfinder versus 16:15 LST for VL- 1), and the 21 years separating the two entry profiles suggests that diurnal and secular effects could be important in understanding their differences.

For an entry vehicle, atmospheric density is directly related to aerodynamic deceleration, velocity relative to the **atmosphere**, and aerodynamic characteristics(2). Deceleration was measured directly; velocity and position can be reconstructed by integrating the equations of motion using the observed decelerations and an initial velocity and position, and Pathfinder entry vehicle aerodynamic characteristics are known **from** computational aerodynamic simulations and laboratory experiments.

Atmospheric densities measured by Pathfinder varied from $5 \times 10^{-11} \text{ kg/m}^3$ at the threshold of detection to $8 \times 10^{-3} \text{ kg/m}^3$ immediately before parachute release at 9 km (Fig. 1). From 160 km to 90 km densities range from a factor of 5 lower than VL- 1 values near and above 120 km to a factor of 2.5 lower near 90 km altitude. The increase in density between 90 and 80 km, which corresponds to a deep temperature minimum (Fig. 2), raises the Pathfinder densities at lower altitudes to values slightly lower than VL- 1 densities. The lower values of density, and therefore **pressure, encountered by Pathfinder below** 30 km are generally consistent with the lower overall mass and surface pressure of the **martian** atmosphere at the time of the Pathfinder landing (11). The decreased surface pressure results from the annual variation in atmospheric mass caused by condensation and sublimation from the polar caps (12).

The **martian** thermosphere, where temperature **increases** rapidly with altitude due to heating by solar EUV radiation, is evident above 125 km in the Pathfinder profile (Fig. 2). Although the uncertainties in the derived temperatures at these altitudes are large, it appears that Pathfinder temperature are close to or slightly warmer than those measured by VL-1.

From 65 to 125 km, **observed** temperatures were, on average, 20 K colder than those observed by VL-1 (Fig. 2). This contrast is responsible for the lower Pathfinder densities above 90 km. Because radiative time constants reach a minimum in this altitude range, a large response to diurnal forcing is a likely explanation for this difference (13). The temperature minimum of 92 K at 80 km is the lowest temperature ever measured in the **martian** atmosphere and may result from the superposition of waves, such as thermal tides, upon the overall nighttime cooling. Tides propagate from the lower atmosphere with amplitudes that increase with altitude.

At 80 km, the Pathfinder temperature profile is colder than the CO_2 condensation temperature (Fig. 2). The lower temperature may result from supercooling, or from inaccuracies in the vapor pressure curve for CO_2 (14), but it is possible that CO_2 could be condensing at these levels to form high altitude clouds. Observations by the Pathfinder imager (IMP) of sky brightening well before the expected start of dawn may indicate the presence of such clouds, although the substantial morning clouds identified in images of the eastern horizon before sunrise are almost certainly water clouds formed at much lower levels (10).

Below 60 km, temperatures measured by Pathfinder are warmer than those of VL-1 down to 35 km and are similar or slightly cooler at lower altitudes down to 16.5 km (Fig. 2). These differences are consistent with minor variability in dust content, and are also within the amplitudes expected from vertically propagating atmospheric waves such as tides (11). In view of the similar solar forcing, it is not surprising that the Pathfinder and VL-1 profiles are comparable in the lower atmosphere. However, Earth-based, disk-averaged, microwave observations over the past 10-15 years have been used to suggest that the martian lower atmosphere undergoes episodes of cooling, characterized by reduced solar-absorbing dust content and 20 K lower temperatures relative to the conditions observed during the Viking mission (4). The Pathfinder entry profile shows no evidence for significant cooling of the lower atmosphere (Fig. 2), although microwave profiles obtained before and after landing suggested that a cool atmosphere would be found (15). Furthermore, IMP observations yield atmospheric dust opacities of 0.5 (10), comparable to those found by VL-1 at the same season. These opacities are consistent with our temperature profile observations. Finally, it is unlikely that Pathfinder entered a locally dusty and anomalously warm region, as dust opacities remained stable throughout the 30 day primary mission (10).

Below 16.5 km a strong thermal inversion is present in the Pathfinder data, where temperature decreases from 200 K to 181 K at 10 km (Fig. 2). This inversion is at too great an altitude to be the strong thermal inversion in the lowest few kilometers of the nighttime diurnal thermal boundary layer on Mars predicted by radiative-convective models and one-dimensional dynamical boundary layer models (16,17). At the base of the Pathfinder profile, temperature appears to increase with decreasing altitude again and can easily achieve the observed surface temperature, including predicted near-surface thermal inversions, without exceeding the adiabatic lapse rate.

The temperature minimum in the 10 km inversion is well below the condensation temperature of water vapor in the martian atmosphere, assuming that the 10 precipitable micrometers of water derived from IMP measurements is uniformly mixed (10). This inversion may mark the altitude of

clouds seen in IMP images before sunrise (**10**) and near the low-latitude morning terminator in **Hubble** Space Telescope images (**18**), although the height of these clouds is not well known. After sunrise, the clouds burned off rapidly, and the inversion may have **disappeared**. What triggered the formation of a strong temperature inversion is not known, but possible mechanisms include the horizontal **advection** of cooler air at 10 km, and vertically propagating finite amplitude gravity waves excited by surface topography in the strongly **stratified** near-surface nighttime boundary layer (**19**). Once clouds formed, thermal emission from the cloud tops could have enhanced the intensity of the inversion at night.

The Landed Mission.

The pressure, temperature and wind velocity data **acquired** by **ASIMET** during the landed mission allow the variability of the **martian** atmosphere at the Ares **Vallis** landing site to be studied during the mid-summer season on short, daily, synoptic (day-to-day) and seasonal **timescales**. This reveals not only the local properties of the atmosphere and its interaction with the surface, but also more global information on atmospheric dust loading, circulation and the seasonal **CO₂** cycle. Comparisons with **VL-1** data taken at the same time of year can be used to identify longer term climate changes.

Pressure Data

During **sols** 1-30, surface pressure at the landing site underwent substantial daily variations of 0.2 to 0.3 **mbar**, associated primarily with the **large** thermal tides in the thin **martian** atmosphere (**12**) (Fig. 3a). Daily pressure cycles were characterized by a strong semi-diurnal oscillation, with two minima and two maxima per sol, together with **diurnal** and higher-order components, although there was considerable day-to-day variability (Fig. 3b). The presence of a large semi-diurnal tidal oscillation is indicative of significant atmospheric dustiness over broad regions of the planet and over an altitude range of at least 10-20 km (**20**).

A long-term trend in daily-mean pressure was **also** seen. A third order polynomial fit to the data shows that mean pressure fell slowly at the beginning of the period and rose at the end, with a minimum just under 6.7 mbar near Sol 20 (**L_s** - 153°) (Fig. 3a). This time corresponds to the annual deep minimum in the seasonal pressure cycle associated with **CO₂** condensation and sublimation in the polar regions of Mars, and seen previously by both Viking landers (**12**).

The **ASI/MET** pressure sensor detected a variety of relatively short time-scale pressure variations. These ranged from seconds to hours, and had magnitudes of 1-50 μbars . The shorter time-scale variations (< 10-15 minutes) appear to be **correlated** with wind and temperature fluctuations, and tend to be largest during late morning and early afternoon when the boundary layer is most turbulent. The most dramatic pressure features were minima of 10-50 μbar , usually less than a minute in duration, associated with vortices ('dust devils') passing over the lander. A particularly good example was seen during the continuous sampling of Sol 25.

Temperature Data.

ASI/MET measurements revealed the time variability of the near surface temperature profile in the martian atmosphere, and can be **used** to calculate boundary layer parameters that were previously only **estimated** (21).

In common with the single level observations of **VL- 1** at the same season, the diurnal temperature variations at the three Pathfinder levels repeat from day-to-day with a high degree of consistency. The diurnal cycle was sampled particularly well on sol 25 (Fig. 4). For the top mast thermocouple, a typical maximum temperature was 263 K at 14:15 LST, and a typical minimum was 197 K at 05:15 LST, shortly before sunrise. Because of the low density of the **martian** atmosphere, near surface **atmospheric temperatures are strongly influenced by the surface temperature cycle, which is** driven by **solar** heating during the day and infrared cooling at night. For this reason, diurnal temperature extremes at the bottom of the mast exceeded those at the top (Fig. 4). Temperatures at the top of the mast (1.1 m) were greater than those seen at 1.6 m by **VL- 1** by 10 K during the day and 12 K at night, probably because of the lower **albedo** and greater thermal inertia of the surface at the Pathfinder landing site.

The diurnal variation of the vertical temperature gradient was also consistent from day-to-day. At sunrise, the atmosphere is typically stably stratified and cool, dense air lies near the surface (Fig. 5). As the surface warms, the air mass is heated from below. By about **06:30** LST all three mast temperatures are approximately equal, indicating that the near surface atmosphere is neutrally stable, as isothermal and adiabatic lapse rates are indistinguishable over a vertical range of 75 cm. By **07:30** LST, ground heating exceeds the ability of the atmosphere to transfer surface heating by conduction, the temperature gradient reverses, the atmosphere becomes unstable, and convection begins. Turbulent mixing carries heat from the surface and is revealed by large, rapid temperature fluctuations of up to 15 to 20 K observed during the remainder of the morning and early afternoon. Later in the afternoon, the surface cools, and turbulent mixing diminishes (Fig. 4), By **16:45** LST

the thermal profile is neutral and what surface winds are observed convect heat quickly. Shortly afterwards, surface cooling causes the temperature gradient to invert and the surface boundary layer becomes stably stratified for the duration of the night, Major nighttime temperature fluctuations are caused by downslope winds that disturb the surface boundary layer (Fig. 4).

Large near surface temperature gradients of 10 to 15 K are probably a common feature of the **martian** day time boundary layer. Because of low atmospheric densities, the convective heat flux is unable to cool the surface as efficiently as on Earth, **where** atmospheric fluxes typically remove 80 to 90 percent of the net surface radiative flux under convective conditions.

Wind Data

The **ASI/MET** wind sensor measured wind speed and direction, 1.1 m above the base of the mast. Accurate speed determination **requires** further calibration of the relation between wind speed, air temperature, and sensor hot wire overheat under Mars surface conditions and is not yet available. Here we discuss wind direction and approximate speed based upon azimuthal variations of wire overheat, which are a function of both wind speed and direction.

For sols 1 to 30, wind direction generally rotated in a clockwise *sense* through all the points of the **compass during the course of a martian day (Fig. 6)**. This rotation was not uniform. Winds were consistently from the south **in** the late night and **early** morning hours, and then rotated steadily through west, north, and east during the day. Over the 30 day period studied, nighttime wind direction was remarkably constant, but considerably more scatter was seen during the day (Fig. 6). The most anomalous wind variations were observed on Sols 8-10, where northeasterly winds **were** absent from the daily cycle. A pronounced **reduction** in the daily variation of surface pressure is seen in the same time interval (Fig. 3).

The recurrent southerly wind from late evening through morning is consistent with a drainage flow down Ares **Vallis**, which rises to the south of the lander (1), and the northerly wind seen in the afternoon is indicative of flow up Ares **Vallis**. Although the clockwise rotation of the wind vector agrees with that expected from the westward migrating classical diurnal thermal tide, the **time-**phasing of wind direction throughout the day does not. The classical tidal drive would generate a westerly maximum near 18:00 LST and a southerly maximum at about 12:00 LST. It therefore appears that local topography, or possibly non-classical tides, are controlling the wind direction at the Pathfinder location during mid-summer.

Winds measured at the **VL-1** site at this same season 11 Mars years earlier (1976), were **generally** weak (< 6 m/sec), exhibited a time-averaged northwesterly direction, and were approximately **upslope** during the afternoon and downslope during the night and **early** morning. Increased wind speeds accompanied the increased pressure oscillations seen during the several sois surrounding $L_s = 150$ (22). If the winds are slope driven at this season, the differences between **VL-1** and Pathfinder winds are expected to reflect differences in the magnitude and direction of the slope at the two sites.

Finally, preliminary estimates suggest that wind speeds were comparable with or lower than those measured by **VL-1** at the same time of year. **Speeds** were generally less than 5 to 10 m/s, except during the passage of dust devils, and were often less than 1 m/s in the morning hours. This may be consistent with the lower slope at the Pathfinder site.

Implications of Landed Data.

Synoptic and Seasonal Variations.

Synoptic and seasonal variability in the **martian** atmosphere at the Ares **Vallis** landing site **are** seen most clearly in the pressure data (Fig. 3). In particular, the annual pressure cycle reached a minimum at about sol 20, **corresponding** to the greatest mass of the southern seasonal polar cap (12), although the precise timing of the pressure minimum can be up to 5 sois earlier and one sol later, depending on exactly how the pressure data are analyzed. The Pathfinder minimum appears to have occurred about 6 sois later than that seen during the **first** year at the **VL-1** site (23), which seems to imply more or longer lasting **CO₂** condensation on the south polar cap. Variations from year to year of at least several sois in the timing of the annual pressure minimum were observed by the two Viking landers (24).

Small synoptic amplitude variations of less than 3-4 K in temperature and 20-30 μ bar in pressure are present in the **ASI/MET** data, after both diurnal fluctuations and longer-term trends are removed. Variations of **comparable** magnitude were found in the **VL-1** data for this season; the greatest variance was at relatively long (10-30 Sol) **periodicities** (23, 25). Missing data and the limited temporal extent of the available Pathfinder observations make the estimation of **periodicities** difficult. Based upon the **VL-1** data and **pre-landing** GCM predictions for the Pathfinder site, it is expected that much larger amplitude synoptic variations will begin as the transition to the fall and winter weather regime takes place (23, 11). There is evidence that this is beginning to happen at the end of the Pathfinder pressure record.

Thermal Tides.

For the first 30 days of the landed mission, the **semidiurnal** tide was the most significant component of the daily surface pressure variation (Fig. 7). Its amplitude is generally similar to that found by VL-1 and is consistent with a global dust visible optical depth of order 0.5 (**20**). This value is comparable to that measured by the IMP (10). Given the long vertical wavelengths associated with the semi-diurnal tide, its measured amplitudes further suggest that the dust was deeply distributed in the atmosphere and was not confined to a shallow layer near the surface. This inference is consistent with the dust scale height of about 13 km deduced **from IMP** measurements (**10**), and our entry profiles which show a relatively warm lower atmosphere below 60 km. However, as mentioned earlier, a deeply distributed global dust haze is not consistent with **Earth-**based microwave measurements for this same period (**15**).

The amplitude of the diurnal tide was small and variable. On sols 5 and 9 normalized amplitudes were down to 0.002 (Fig. 7), which is more than a factor of two smaller than anything measured by Viking. The variation seen by Pathfinder is somewhat systematic in that diurnal amplitudes were low during the first 5-10 **sols**, gradually rose to values of around 0.010 by sol 20, then **declined** to rather low values again by sol 27. Phase also varied during this period; retarding during **the first 15 sols, then advancing during the last 15 sols**. The amplitude of the diurnal tide is sensitive to the calibration of the pressure sensor which is still preliminary. However, the time variation of amplitude and phase is relatively insensitive to calibration

These variations in the diurnal tide suggest that it was modulated by interference effects between the sun-following westward tide, and the topographically induced, resonantly enhanced, eastward traveling, diurnal Kelvin mode (20,22,26). One possibility is that the interaction is between eastward and westward modes of comparable amplitude, where the eastward mode period is first slightly greater than and later slightly less than a sol. Alternatively, the eastward and westward modes could have similar periods, and amplitudes may vary with time. The modeling of this interaction may help to distinguish between these two possibilities

Nighttime Temperature Inflections.

ASI/MET temperature measurements show that, on average, atmospheric temperatures fall monotonically through the evening and night until sunrise. On most nights, however, the steady decline in temperature was interrupted by one or more inflections in the gradient, where the

temperature fell less rapidly or even rose before resuming its downward trend. Striking features of this kind are seen in figure 4 at 18:15, 19:00,20:40, and **03:05** LST, and are particularly marked in top mast thermocouple temperatures.

Temperature inflections seen in the VL-1 temperature data set were attributed to radiative effects associated with the formation of ground fogs (27). At the Pathfinder landing site, temperatures are of order 10 K warmer than those of **VL- 1** at night, and condensation is unlikely, given the 10 **precipitable** micrometers of water measured by the IMP (10). However, there was a positive correlation between increased wind speed and the observed thermocouple temperature inflections. Increased horizontal flow may have disturbed the strong temperature inversion that **developed** at night, bringing warmer air from aloft down to thermocouple heights through enhanced vertical mixing. After the nighttime warming episodes, temperatures fell rapidly in conjunction with significant reductions in wind speed. The nighttime temperature inflections occurred in the presence of southerly winds, and can not be produced by thermal contamination from the body of the spacecraft which is located to the northwest of the MET mast.

Dust Devils.

Short term variations in measured surface pressure, wind velocity, and air temperature, over periods of tens of seconds to minutes suggest that small scale convective vortices passed through the Pathfinder lander site. During the passage of one of these features, pressure fell and recovered rapidly accompanied by abrupt shifts in wind direction. These events, which we refer to as ‘dust devils’, are probably similar in character to features noted in the **VL-1&2** meteorology data (28), and may have been seen by the Viking orbiter cameras (29). The narrow, well **defined** pressure minimum is the most characteristic feature of these vortices, but it was not seen in the Viking lander pressure record because of poor resolution and coarse temporal sampling. There are currently no Pathfinder lander images to indicate whether the apparent vortices entrain dust, but the passage of a particularly large feature on sol 62 was **correlated** with a short-lived reduction of about 1.5 percent in the power generated by the Pathfinder solar panels.

A dust devil event at 14:15 LST on Sol 25 has the characteristics of a clockwise rotating vortex traveling toward the south-southeast (1600), with the vortex center passing west and south of the lander (Fig. 8). During this event, pressure fell 0.028 mbar in 24 s to a minimum, followed by a more rapid **rise** of 0.027 **mbars** in 8 s. The pressure minimum was accompanied by a local temperature maximum at all three thermocouple heights. These temperature maxima are themselves embedded in a pronounced temperature minimum which extended 30 to 40 s before and after the

pressure minimum. Wind direction **rotated** from northwesterly, the mean flow direction **prior** to the vortex arrival, through north to northeasterly in the 40 seconds preceding the pressure minimum, before shifting abruptly through northerly to westerly at and just after the pressure minimum. Wind direction slowly returned to north-northwesterly over the minutes following the pressure minimum. This pattern is consistent with a clockwise rotating vortex embedded in an ambient flow which has a speed less than the vortex rotational speed (28).

Boundary Layer Results

The near surface boundary layer of the **martian** atmosphere can be described by ‘universal’ scaling laws, involving dimensionless coefficients determined from measurements in the Earth’s atmosphere. The Viking and Pathfinder measurements provide us with an opportunity to test this universality using measurements in another atmosphere. Although the Martian atmosphere differs in many respects from our own, most of the universal relations are expected to be valid, based on the analysis of Viking data (30).

Relative to Viking, the Pathfinder measurements have the following advantages for boundary layer studies. Temperature measurements at several heights allow for a more direct determination of the vertical temperature gradient, and the successful MET sampling strategy has ensured that high temporal resolution (1 Hz or better) turbulence and profile data are available over a wide variety of conditions with good systematic coverage of diurnal and **interdiurnal** variability.

As an example of the analysis of turbulence characteristics from Pathfinder, we show temperature power spectra obtained from night and daytime data by the Fourier decomposition of temperature time series (Fig. 9). These spectra are scaled by the appropriate temperature scale, T^* , which, following the **Monin-Obuchov** formulation, is the most important scaling parameter for both vertical profiles and spectra (30). The T^* values scaling the spectra, were derived from the measured temperature gradients, assuming close to neutral thermal stability due to the proximity of the ground (**0.25m**), although T^* ranges from -5 K to +0.2 K. Although simplified, the scaling does a reasonable job in collapsing the data, and hence in supporting the applicability of the **Monin-Obuchov** scaling laws.

References and Notes

1. **M.P. Golombek et al.**, *This Issue*.
2. **A. Seiff et al.**, *J. Geophys. Res.* 102,4045 (1997).
3. **A. Seiff and D.B. Kirk**, *J. Geophys. Res.* 82,4364 (1977).
4. **R.T. Clancy et al.**, *Icarus* 122, (1996).
5. **S.L. Hess, R.M. Henry, C. B. Leovy, J. A. Ryan, J.E. Tillman**, *J. Geophys. Res.* 82, 4559 (1977).
6. **W.M. Folkner, C. F. Yoder, D. N. Yuan, E. M. Standish, R.A. Preston**, *This Issue*.
7. **W.M. Folkner**, Private Communication.
8. **T. Riven et al.**, *J. Spacecraft Rockets* 34,265 (1997).
9. **A.O. Nier and M.B. McElroy**. *J. Geophys. Res.* 82,4341 (1977).
10. **P.H. Smith et al.**, *This Issue*.
11. **R.M. Haberle, J.R. Barnes, J.R. Murphy, M.M. Joshi, J. Schaeffer**. *J. Geophys. Res.* 102, 13301 (1997).
12. **R.W. Zurek et al.**, in *Mars*, **H.H. Kieffer, B.M. Jakosky, C.W. Snyder, M.S. Matthews**, Eds. (Univ. of Arizona Press, Tucson, 1992), pp. 835-933.
13. **M. Lopez-Puertas and M.A. Lopez-Valverde**. *Icarus* **114**, 113 (1995).
14. **P.B. James, H.H. Kieffer, and D.A. Paige**, in (12), pp. 934-968.
15. We would like to thank **Todd Clancy for supplying unpublished microwave profiles to the ASI/MET team** within days of the original observations.
16. **P. J. Gierasch and R. M. Goody**. *Planet. Space Sci.* 16,615 (1968).
17. **R.M. Haberle, H.C. Houben, R. Hertenstein, T. Herdtle**. *J. Atmos. Sci.* 50, 1544 (1993).
18. **M.J. Wolff, R.T. Clancy, P.B. James, S.W. Lee, J.F. Bell III**. *Bull. Amer. Astron. Soc.* In Press (1997).
19. **J.A. Magalhães and R.E. Young**. *Icarus* 113,277 (1995).
20. **R.W. Zurek and C.B. Leovy**. *Science* 213,437 (1981).
21. **J.L. Sutton, C.B. Leovy, J.E. Tillman**. *J. Atmos. Sci.* 35, 2346 (1978).
22. **J.E. Tillman**. *J. Geophys. Res.* 93,9433 (1988).
23. **J.R. Murphy, C.B. Leovy and J.E. Tillman**. *J. Geophys. Res.* 95, 14555 (1990).
24. **J.E. Tillman, N.C. Johnson, P. Guttorp, D.B. Percival**, *J. Geophys. Res.* 98, 10963 (1993).
25. **R.D. Sharman and J.A. Ryan**. *J. Atmos. Sci.* 37, 1994 (1980).
26. **R.J. Wilson and K. Hamilton**. *J. Atmos. Sci.* 53, 1290 (1996).
27. **B.M. Jakosky, A. P. Zent, R. W. Zurek**. *Icarus* In Press (1997).

28. **J.A. Ryan** and **R.D. Lucich**. *J. Geophys. Res* 88, 11005 (1983).
29. P. Thomas and **P.J. Gierasch**. *Science* 230, 175 (1985).
30. **J.E. Tillman**, L. Landberg, **S.E. Larsen**. *J. Atmos. Sci.* 51, 1709 (1994).

Figure Captions

Fig. 1. The atmospheric density profile derived from the Mars Pathfinder atmospheric structure investigation. The solid lines give the mean atmospheric density profile derived from the accelerometer data and profiles reflecting ± 2 -sigma uncertainties in density based on uncertainties in the entry velocity and the finite digital resolution of the instrument. Errors in aerodynamic characteristics are not included, but are not expected to change the error envelopes substantially. Further work with the accelerometer and pressure data will allow us to extend the density profile down to the surface where the MET observations of pressure and temperature indicate an atmospheric density of $1.76 \times 10^{-2} \text{ kg/m}^3$ marked by a circle in the figure. Results from the VL- 1 Atmospheric Structure Instrument (AS I) (2) and the Viking 1 Upper Atmosphere Mass Spectrometer (UAMS) are also plotted for comparison (Dashed lines) (2).

Fig. 2. The atmospheric temperature profile derived from the Mars Pathfinder atmospheric density profile. Temperature profiles corresponding to the nominal and ± 2 -sigma density profiles of figure 1 are represented by solid lines. The hydrostatic equation is integrated to derive a pressure profile from the density profile, and temperature is calculated from density and pressure using the ideal gas law. To begin the integration, an upper boundary temperature is determined from the density scale height at the upper boundary. Uncertainties in this temperature only affect the derived profiles significant y above 125 km. In order to derive temperatures, we have constructed a molecular weight versus atmospheric density model based on the results of the Viking Upper Atmosphere Mass Spectrometer (9). At present we have no way of quantifying the accuracy of this model which influences temperature above 120 km. At lower altitudes the martian atmosphere is well-mixed with a constant molecular weight of 43.49. Temperature profiles from the VL- 1 AS I and UAMS experiments ((2), Dashed lines), the CO₂ condensation temperature profile (Dotted line), and the surface temperature measured by the Pathfinder MET instrument (Circle) are also shown for comparison.

Fig. 3. a. Time-averaged surface pressures measured by the MET instrument over the first 30 days of the Pathfinder landed mission. The averages are primarily over the three-minute default measurement sessions, of which there are nominally 51 per sol, and the resulting points have been connected with straight lines, except for sols 12-15 where cubic spline interpolation has been used to fill data gaps of about 8 hours in length. MET operation was restricted to nighttime observations during this period to prevent spacecraft resets associated with MET data collection. The major gaps in the data set at Sols 1, 8, 11, & 17 are caused by various spacecraft software reset and downlink problems. After Sol 17, the reset problems associated with MET were corrected and continuous

sampling was resumed. The long-term trend in pressure has been represented by a third-order polynomial fit to the data (Solid curve). b. Diurnal pressure cycles for Sols 9 (Solid line) and 19 (Dashed line), illustrating the observed day-to-day changes in the diurnal pressure cycle and allowing details of the daily pressure variation to be seen **more** clearly.

Fig. 4. The diurnal variation of atmospheric temperature measured by the top (red), middle (green), and bottom (blue) mast thermocouples, from **06:00** LST on sol 25 to **06:00** LST on sol 26. These thermocouples are respectively 100, 50, and 25 cm above the plane of the lander solar panels. Temperatures are sampled continuously at four second intervals throughout this **period**, but the plots use 30 point (2 minute) running means for clarity. (**NB.** This smoothing reduces the amplitude and frequency of the fluctuations present in the raw data).

Fig. 5. The data of figure 4 plotted as temperature deviations from the mean of all three thermocouples. Sampling times and data smoothing are identical to those of figure 4.

Fig. 6. Time-averaged wind direction measured by the MET instrument over the first 30 days of the Pathfinder landed mission plotted as a function of local solar time. Each point represents an average over a three-minute default measurement session. Wind direction is defined as follows: 0 and 360 degrees (northerly), 90 degrees (easterly), 180 degrees (southerly), and 270 degrees (**westerly**).

Fig. 7. a. The amplitude of the diurnal (black diamonds) and **semidiurnal** (open diamonds) surface pressure tides for the first 30 days of the Pathfinder landed mission. Amplitudes are normalized relative to the mean pressure for each day. b. The phase, in LST, of the diurnal (black diamonds) and **semidiurnal** (open diamonds) surface pressure tides. Enough pressure data were collected to characterize the thermal tide on 20 **sols**. **Pressure** measurements from each of these **sois** were fitted with a cubic **spline**, from which 51 equally spaced intervals were sampled to define the tide.

Fig. 8. Pressure, wind, and temperature changes associated with a small-scale vortex, or dust devil, passing through the Pathfinder landing site. The measurements are taken at four second intervals

Fig. 9. Composite plot of night-time and day-time power spectra $S(f)$ for 10 minute martian atmosphere temperature time series from the bottom mast thermocouple. The spectra are normalized by the turbulence temperature scale T^* derived from the temperature profiles, assuming a logarithmic profile of $T(z) = T^*/\kappa \ln(z/z_0)$, and plotted versus the frequency f . The spectra

(fine lines) and **their average** (dashed **line**) **are compared** to a **similar spectrum from Earth** obtained under weakly unstable conditions (Bold line). The difference between the Earth and Mars spectra at high frequencies is mainly due to sensor time constants. The "**2/3**" line represents the ideal inertial subrange power law slope.

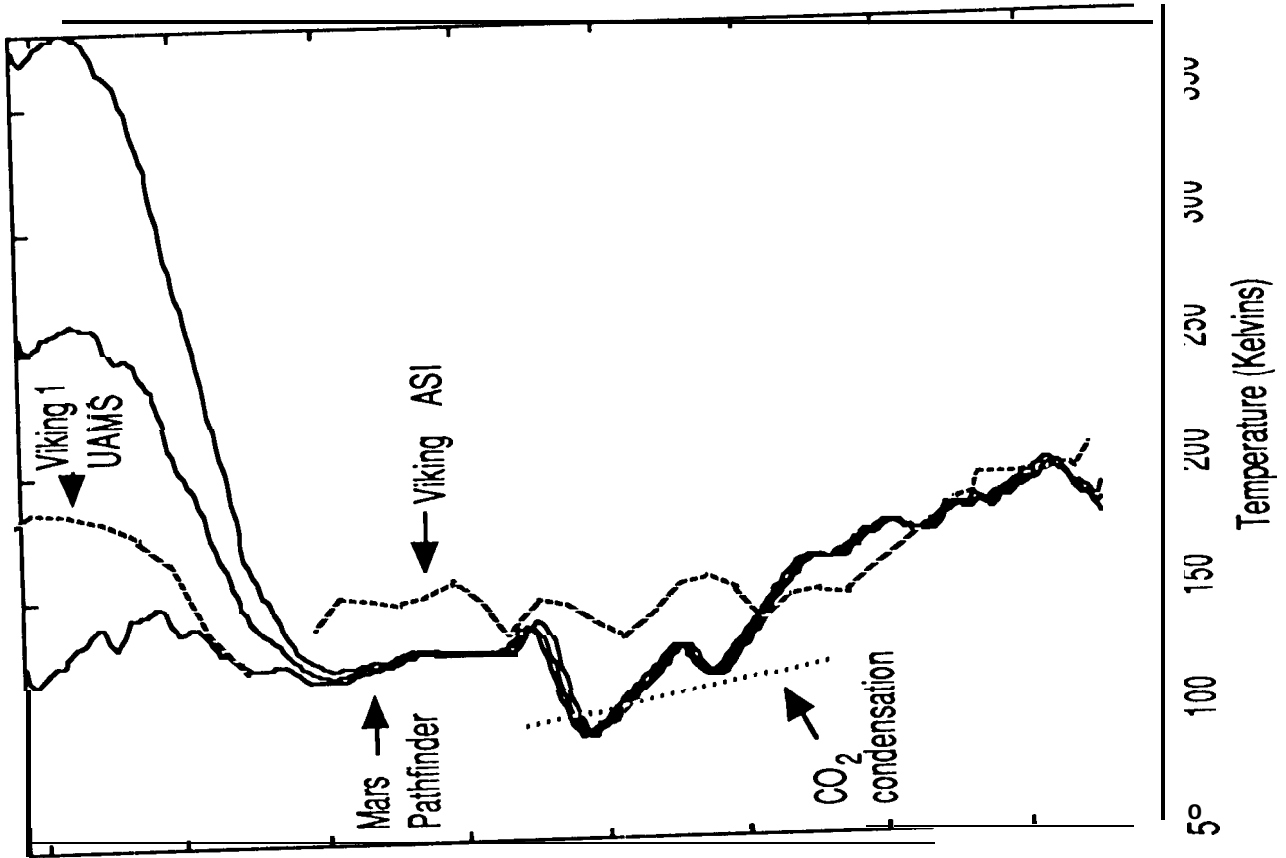


Figure 7

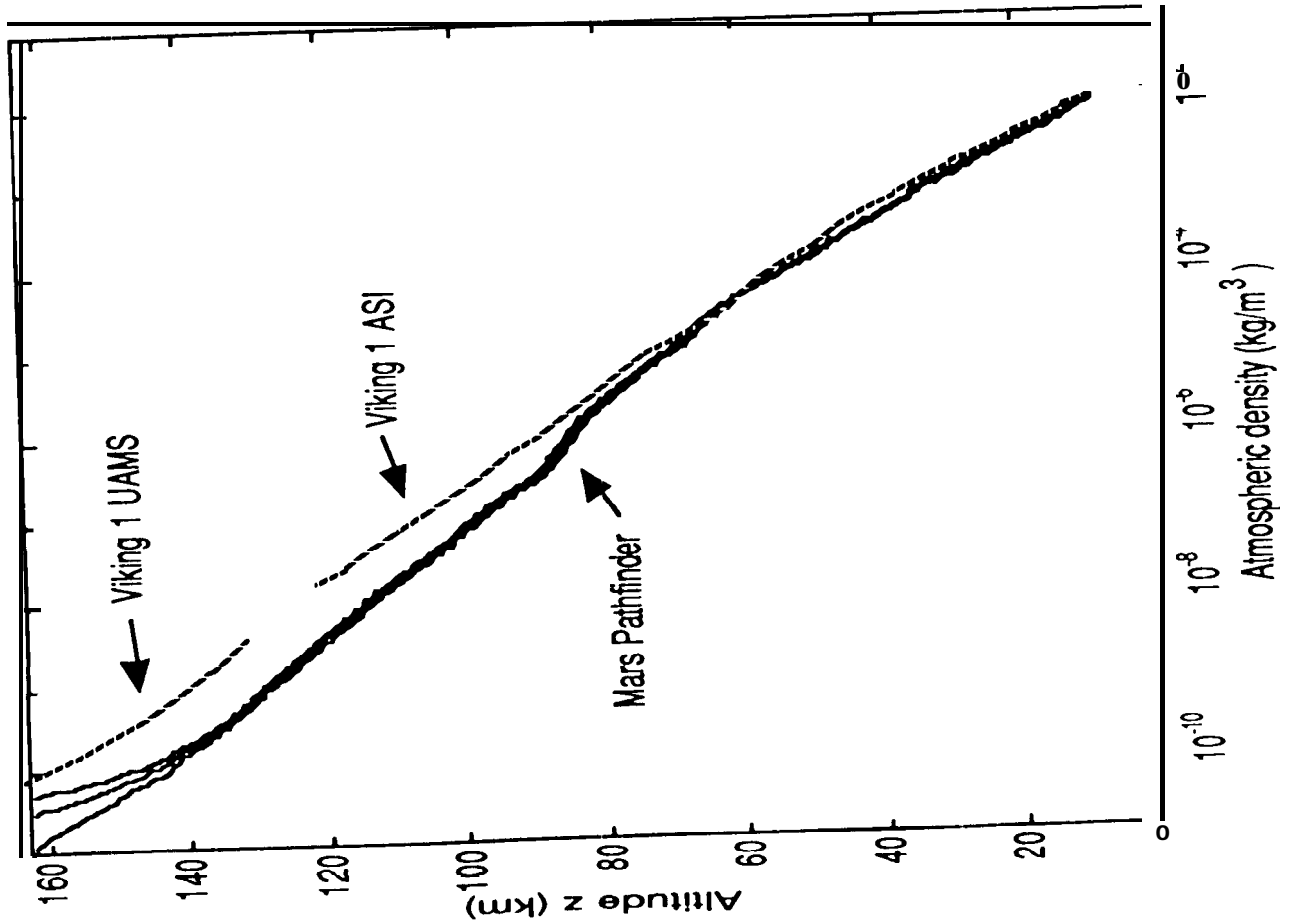


Figure 1

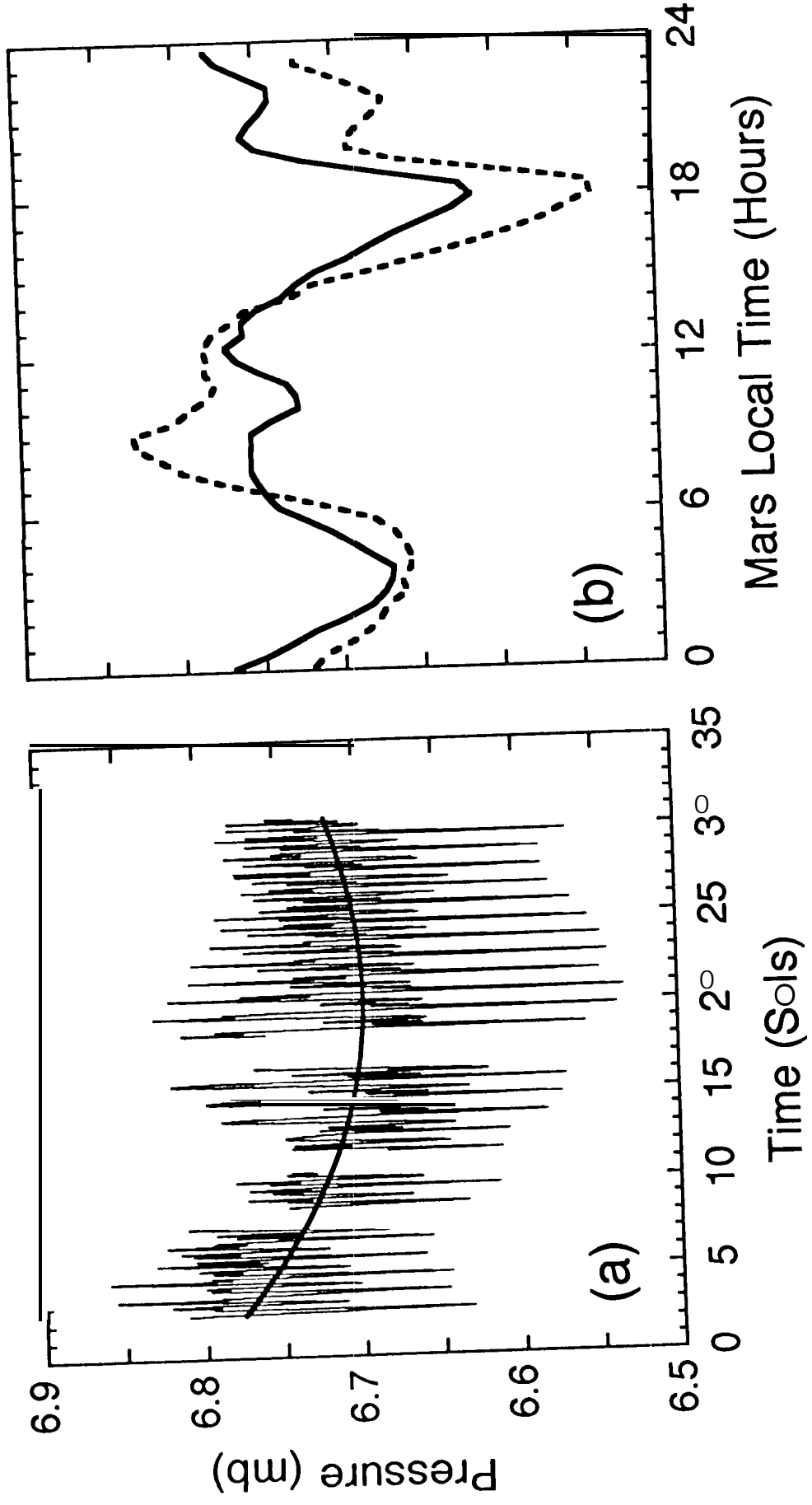


Fig 4

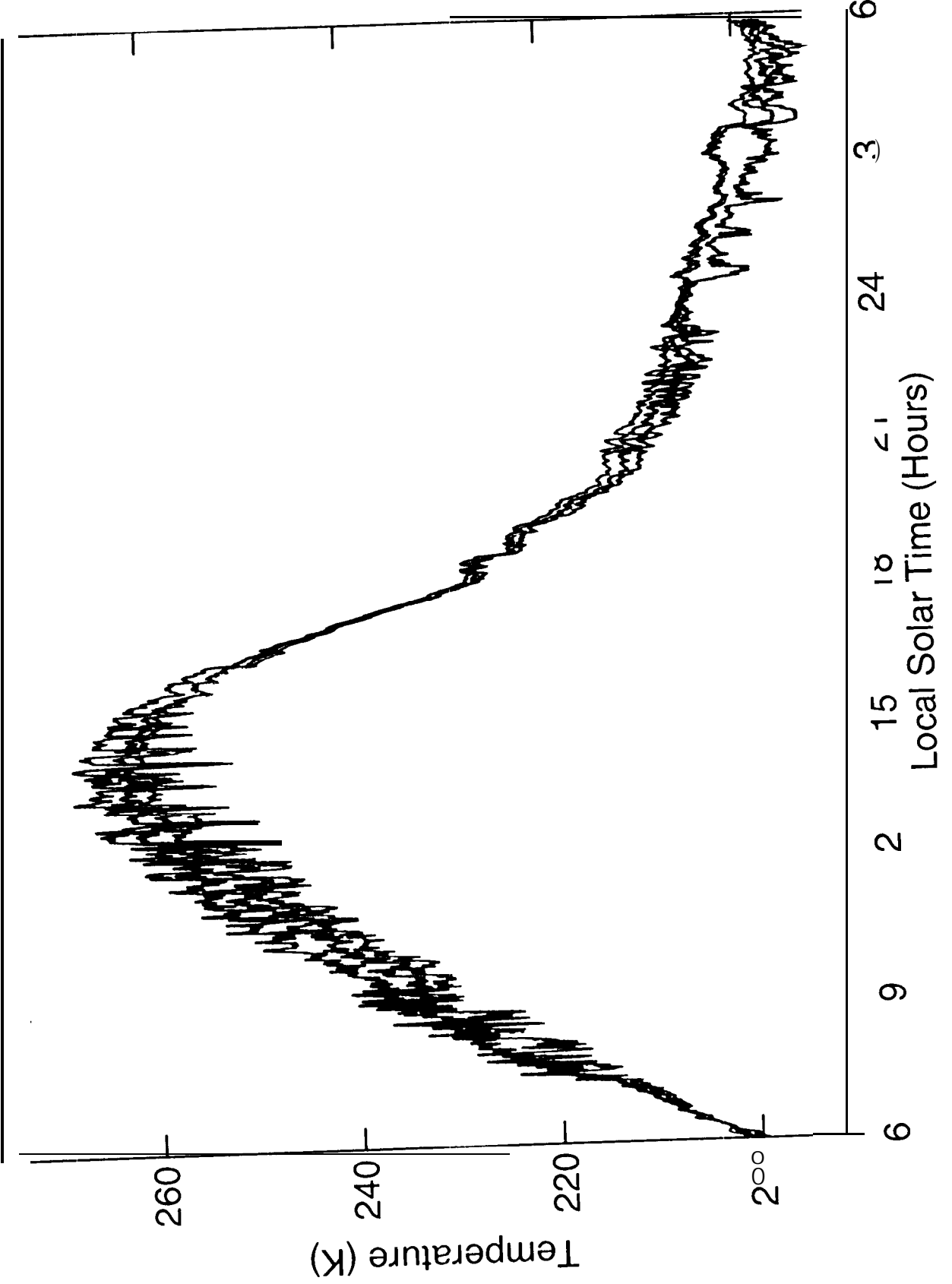


Fig 5

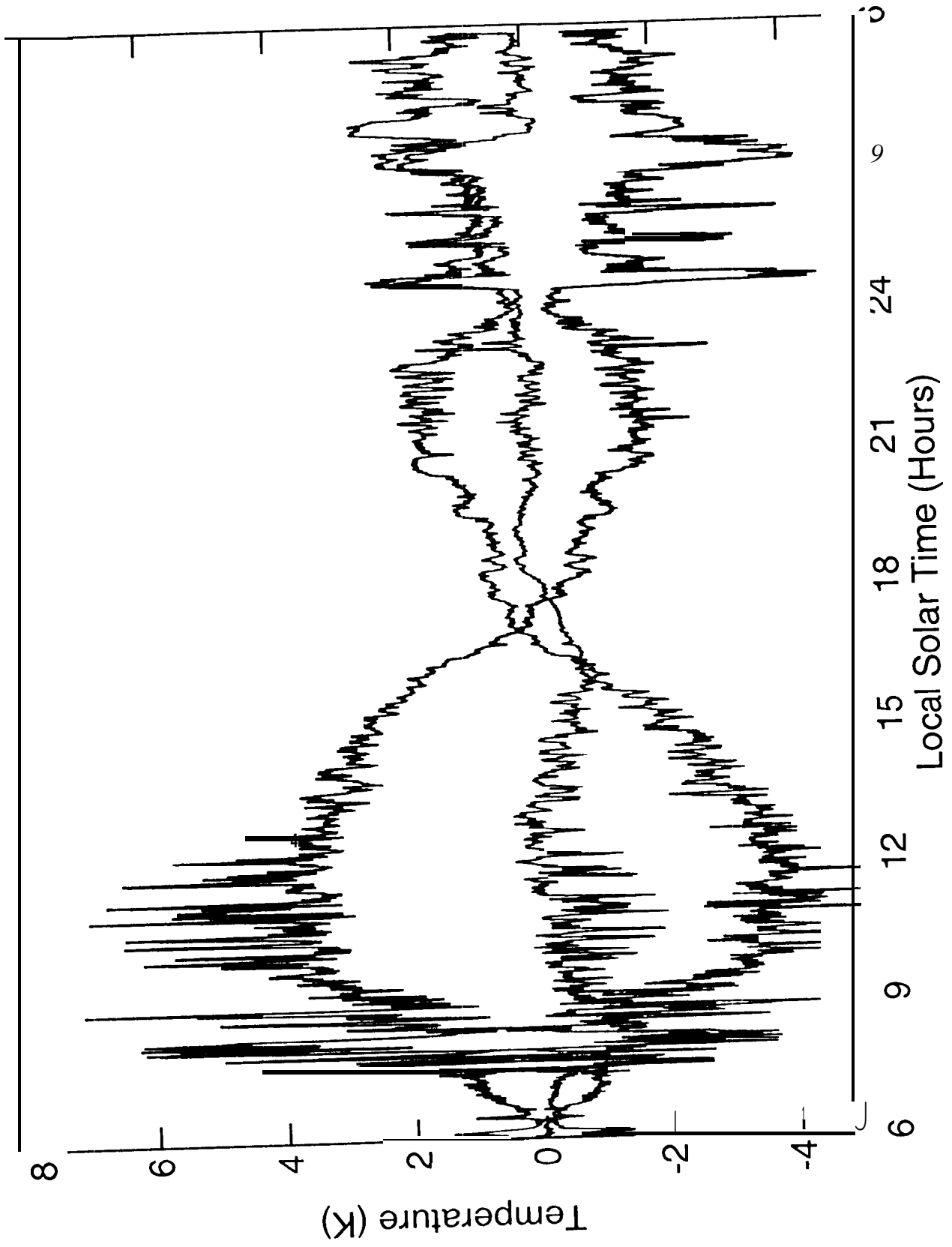


Figure 6

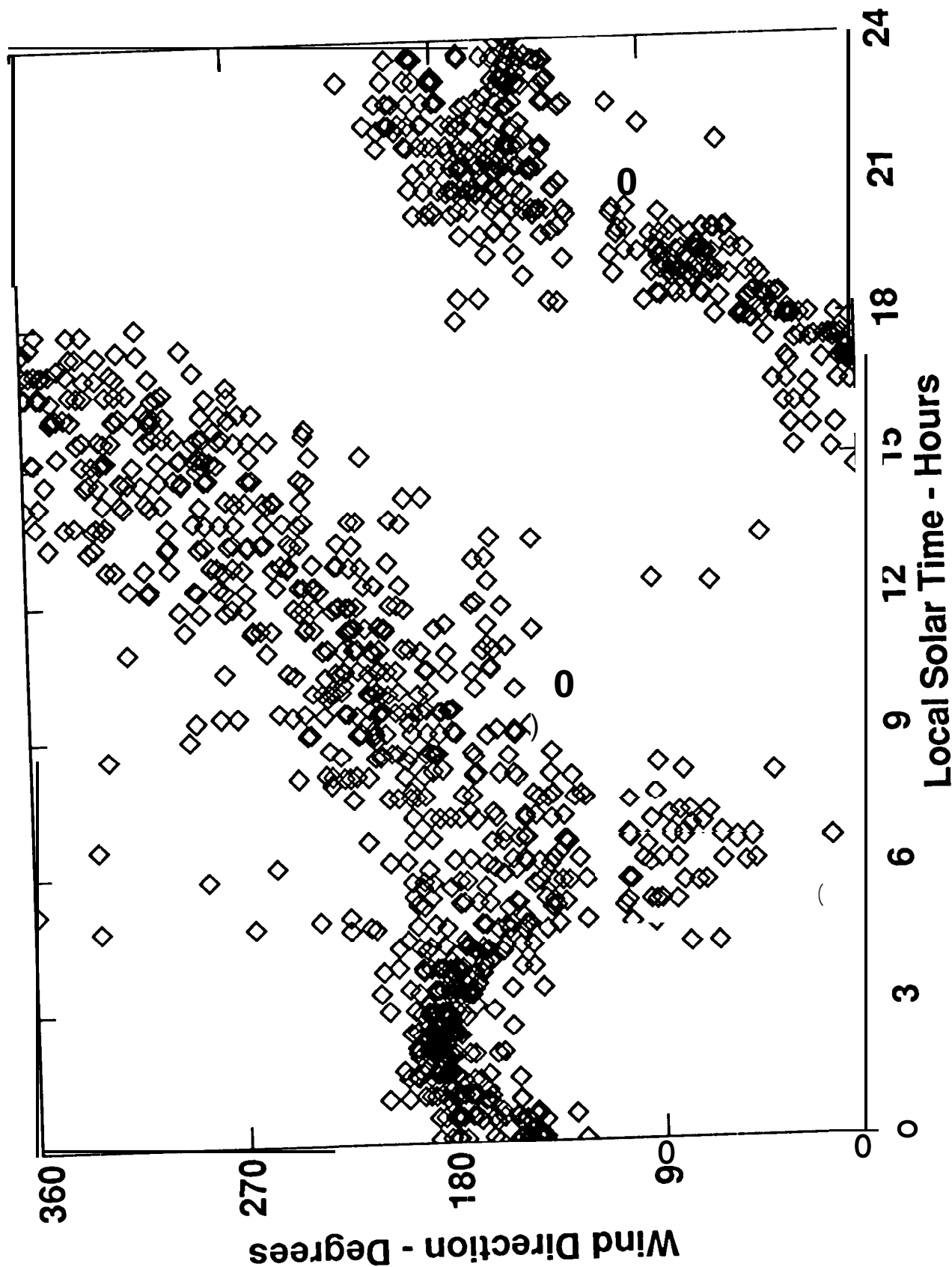
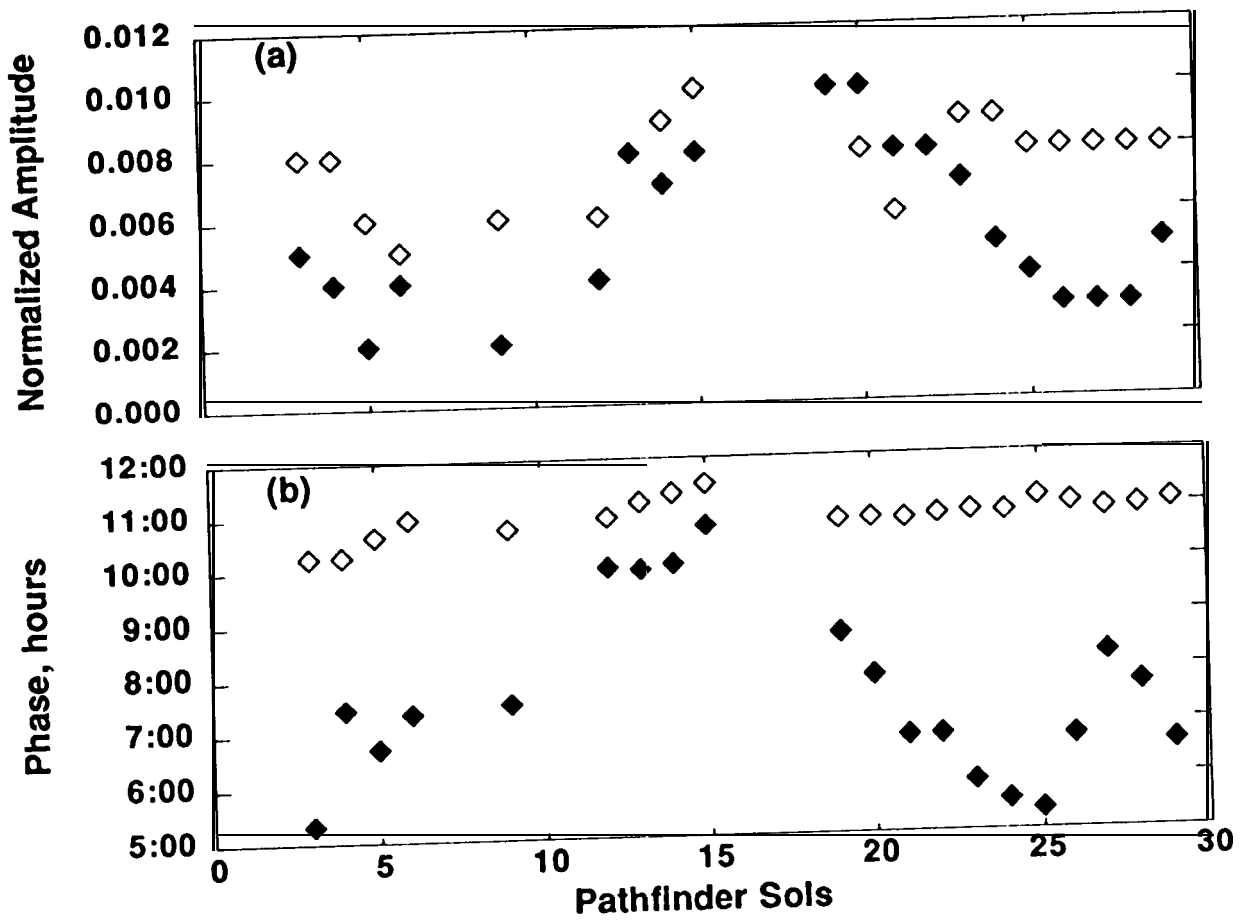


Figure 7



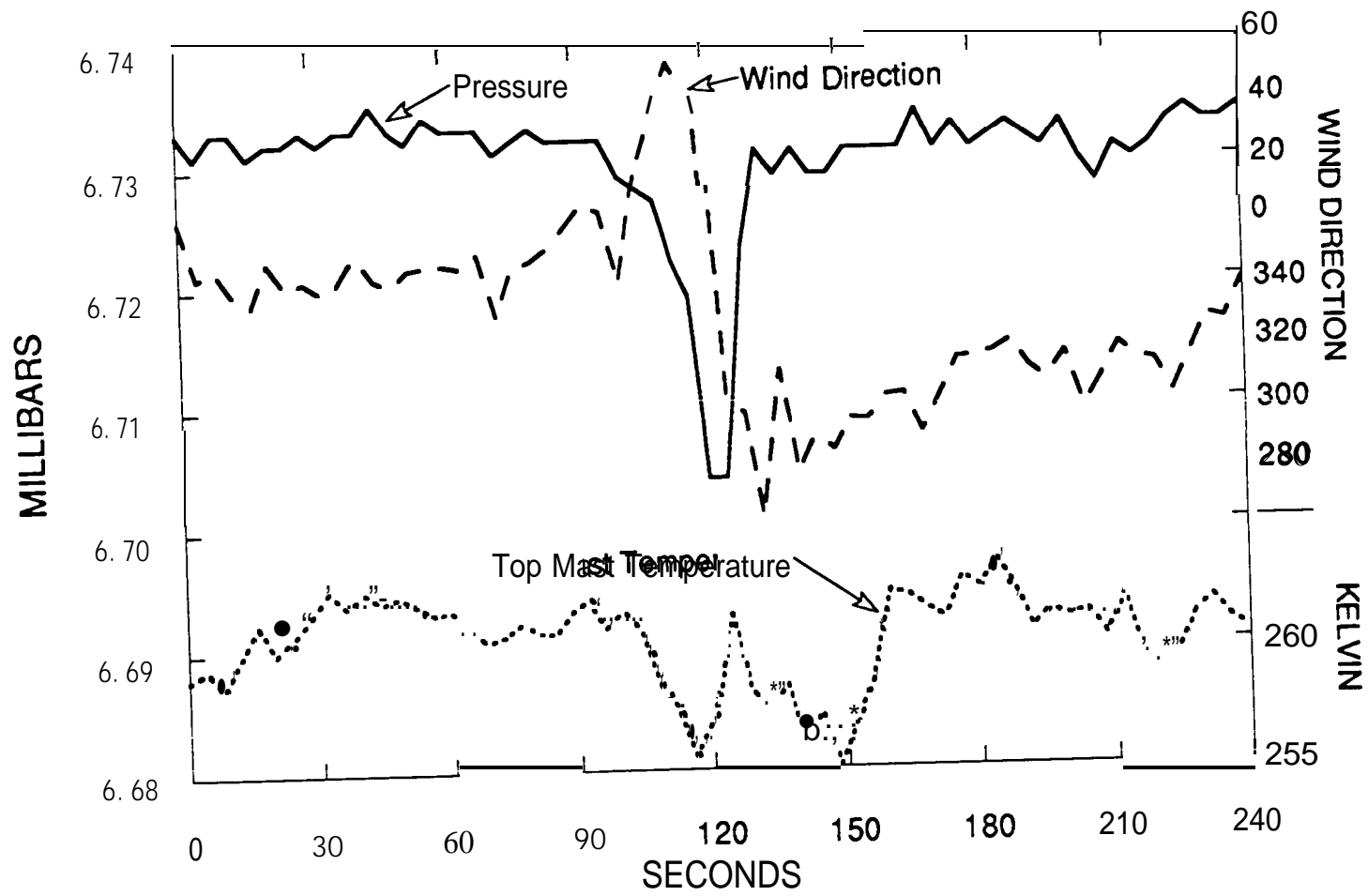


Figure 8

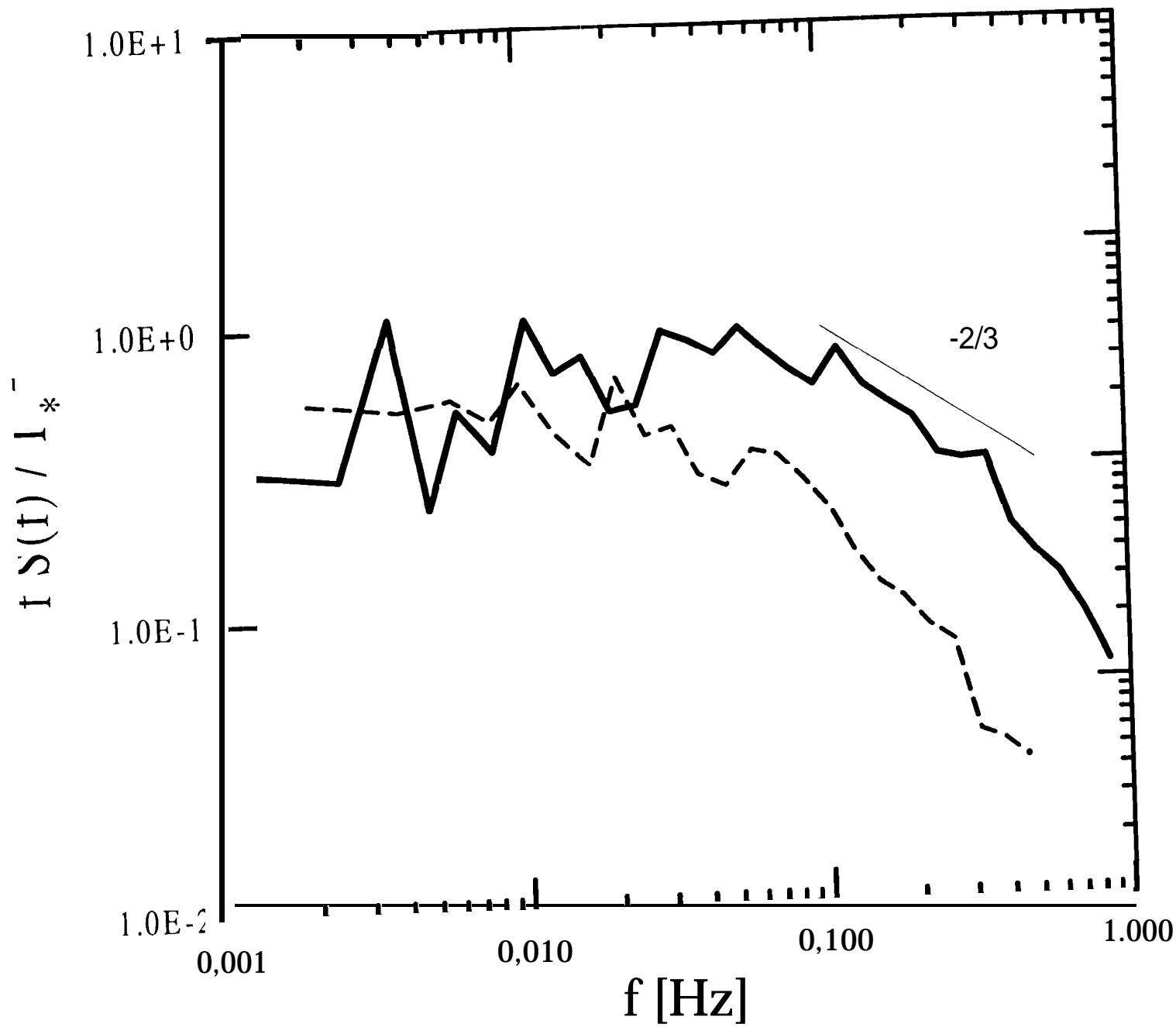


Figure 9